

Innervation density and types of nerves in prostate cancer

Filip BLASKO^{1,2}, Lucia KRIVOSIKOVA³, Pavel BABAL³, Jan BREZA⁴, Branislav TREBATICKY⁵, Roman KURUC⁶, Boris MRAVEC^{1,2}, Pavol JANEGA³

¹Institute of Physiology, Faculty of Medicine, Comenius University in Bratislava, Bratislava, Slovakia; ²Biomedical Research Center, Institute of Experimental Endocrinology, Slovak Academy of Sciences, Bratislava, Slovakia; ³Institute of Pathological Anatomy, Faculty of Medicine, Comenius University in Bratislava, Bratislava, Slovakia; ⁴Department of Pediatric Urology, Faculty of Medicine, Comenius University in Bratislava, Bratislava, Slovakia; ⁵Department of Urology, Faculty of Medicine, Comenius University in Bratislava, Bratislava, Slovakia; ⁶Health Care Surveillance Authority of the Slovak Republic, Bratislava, Slovakia

*Correspondence: lucia.krivosikova@fmed.uniba.sk; pavel.babal@fmed.uniba.sk

Received November 16, 2023 / Accepted December 20, 2023

Innervation of cancerous tissue represents an important pathway enabling the nervous system to influence the processes associated with the initiation, progression, and metastasis of a neoplastic process. In the context of prostate cancer, several papers report the presence of innervation and its modulating effect on the cancer prognosis. However, most of the data are experimental, with limited information on human prostate cancer innervation. Morphometric analysis of archival prostate specimen immunohistochemistry with neural markers PGP9.5 and S100 showed a significant decrease of nerve density in the prostate cancer (n=44) compared to the normal prostate tissue (n=18) and benign prostatic hyperplasia (n=28). Sympathetic nerves were detected with TH, parasympathetic with VACHT, and sensory nerves with SP and CGRP protein detection. Dual immunofluorescence revealed numerous sympathetic nerves in normal prostate and benign prostatic hyperplasia, especially in the peripheral parts. Only a few parasympathetic nerves were found between the glands and in the peripheral parts of the prostate and benign hyperplasia. Sporadic positivity for sensory innervation was present only in approximately 1/10 of nerve fibers, especially in the larger nerves. The pattern of innervation in prostate cancer was analogous to that in normal prostate gland and benign prostatic hyperplasia but there was a significantly lower amount of all nerve types, especially in high-grade carcinoma cases. Although not significant, there was a tendency of decreasing innervation density with increasing Gleason score. Regarding the low density of nerves in prostate carcinoma, the significantly lower PCNA counts in nerves of the cancer specimens cannot be ascribed to lower proliferation activity. Our data confirmed the lower nerve density in the prostate cancer compared to the benign prostate tissue. We could not approve an increased nerve proliferation activity in prostate cancer. All nerve types, most the sympathetic, less the parasympathetic, and the sensory nerves, are present in prostate cancer. The highest nerve density at the periphery of the cancer tissue implies this to be the result of an expansive tumor growth. It is evident that the results of experimental prostate cancer models can be applied to human pathology only to a certain extent. The relation between the range of innervation and the biology of prostate cancer is very complex and will require more detailed information to be applied in therapeutic solutions.

Key words: neurobiology of cancer; cancer innervation; sympathetic nerves; parasympathetic nerves; sensory nerves; prostate cancer; benign prostatic hyperplasia

Prostate cancer is the second most commonly diagnosed type of cancer in men, and a significant contributor to cancer-related mortality [1, 2]. Mortality associated with prostate cancer often results from progression to treatment-resistant neuroendocrine prostate cancer. Perineural invasion in prostate cancer is a well-recognized process associated with a more aggressive tumor phenotype [3, 4].

The human prostate is innervated by sympathetic and parasympathetic nerve fibers arising from the inferior hypogastric plexus [5]. Accumulating data indicate that,

in addition to perineural invasion, interactions between nerves and prostate cancer cells are bidirectional and highly complex [6] and influence processes associated with the initiation, progression, and metastasis of prostate carcinoma [7–9]. Combined neuroscience and oncology research, the neurobiology of cancer, has revealed several mechanisms and pathways by which the sympathetic, parasympathetic, and sensory peripheral nerve fibers innervating tumors affect cancerous tissue [10]. Available experimental and clinical data indicate that one of the important diagnostic



and prognostic factors, in monitoring the influence of nerve fibers on tumors, is the density of tumor innervation or the number of nerves identified in a specific area [11]. In general, higher nerve density has been suggested to correlate with worse prognosis in patients with prostate cancer [7, 12, 13]. However, there are papers describing the low density of innervation in high-grade prostate carcinoma, and therefore the relationship between nerve density and prognosis in oncological patients is not fully understood [14]. Based on these findings, tumor innervation is considered another fundamental characteristic of cancer and an important prognostic marker with expected therapeutic potential [3, 7].

Information on the innervation of the human prostate is limited and generally based on experimental data. Therefore, we decided to determine the innervation density and evaluate the differences in innervation between the healthy prostate gland and diseases of the prostate (benign prostatic hyperplasia, prostate cancer). We also investigated the phenotype of innervation (sympathetic, parasympathetic, sensory) in representative specimens of prostate gland, benign prostatic hyperplasia, and prostate cancer. In addition, we quantitatively evaluated the proliferative activity of nerves in different pathologies of the prostate tissue.

Patients and methods

Patients and specimens. Archival paraffin-embedded prostate needle biopsies (from 18 patients) and open prostatectomy specimens (from 29 patients) were used. From each patient, 1 representative paraffin block of prostate carcinoma (PCa) and 1 of the benign prostatic hyperplasia (BH) were selected. For BH, only those samples were selected that did not contain cancer cells (n=28). In prostate cancer specimens (n=44), Gleason score was determined according to the International Society of Urological Pathology 2005 modified Gleason grading system. As controls, we used samples from the necropsy material of the Health Care Surveillance Authority of the Slovak Republic (n=18) of younger men (age range 16–39 years). All autopsies were performed within 23 hours after death. Only patients without pathological findings in the prostate were selected. All specimens were fixed in 10% neutral formalin, routinely processed into paraffin blocks, and stained with hematoxylin and eosin (BD Bamed, Czech Republic).

Immunohistochemistry. For evaluation of innervation density, nerve type, and quantitative analysis of nerve proliferation by immunohistochemistry, 4 µm thick tissue sections were deparaffinized, rehydrated, and processed for antigen retrieval at 96°C in 10 mmol/l citrate buffer (pH 6) for 30 min in the Dako PT-Link chamber (Dako, Glostrup, Denmark). Immunostaining was performed using the Dako Autostainer (Dako).

Nerve density. First, we tested the immunohistochemical detection of nerve fibers using antibodies against protein gene product 9.5 (PGP9.5) and against protein S100. Based

on the test results, we preferred the detection of nerve structures by protein S100 immunostaining due to the frequent PGP9.5 immunoreactivity in epithelial cells. For peripheral nerves detection, the slides were incubated for 1 h with rabbit polyclonal antibody to protein S100 diluted 1:800 in Antigen Diluent (Agilent Technologies, St. Clara, CA, USA) followed by incubation for 30 min with Simple Stain Universal Immuno-Alkaline Phosphatase Polymer-conjugated secondary antibodies (anti-rabbit and anti-mouse; Nichirei Biosciences, Japan) and the reaction was developed with alkaline phosphatase substrate ImmPACT Vector Red (Vector Laboratories, Burlingame, CA, USA). Slides were counterstained with hematoxylin (BD Bamed, Czech Republic), mounted in a water-based Fluorescence Mounting medium (Agilent), and examined with an Eclipse 80i microscope (Nikon, Tokyo, Japan).

Histomorphometry. Nerve area in pixels was measured in digitized 4 random microscopic fields from each sample at 10x magnification using the ImageJ morphometric software version 2.14.0 (National Institutes of Health, USA). H&E DAB vectors were used for color deconvolution. The total area of nerves was determined by the ratio of the red color (S100 expression in nerves) to the total area of the image. The measured pixels of S100 protein expression were then converted to area percentages and used to evaluate the density of nerves in the prostate gland, benign prostatic hyperplasia, and prostate cancer specimens.

Types of nerve fibers. To determine the phenotype of innervation, combined immunofluorescence staining was performed on selected representative specimens of the different pathologies of the human prostate: healthy prostate gland – CON (n=5), benign prostatic hyperplasia – BH (n=10), low-grade prostate cancer with Gleason pattern 3 – LG PCa (n=5), and high-grade prostate cancer with Gleason patterns 4 and 5 – HG PCa (n=5). After antigen retrieval as described above, tissue sections were incubated with primary antibodies for 1 h in a humid chamber at room temperature. Antibodies to common neuronal markers, mouse monoclonal antibody to protein gene product 9.5-PGP9.5 (ab8189, Abcam, Cambridge, UK), diluted 1:500 in Antigen Diluent (Agilent), and rabbit polyclonal antibody against S100 protein (ab34686, Abcam) diluted 1:800, were combined with primary antibodies against specific nerve type markers: antibodies against tyrosine hydroxylase – TH (1:1000; rabbit polyclonal antibody; AB152, Merck, Darmstadt, Germany) for sympathetic nerve detection; vesicular acetylcholine transporter – VAcHT (1:1000; rabbit polyclonal antibody; Cat. No.: 139 103, Synaptic Systems, Göttingen, Germany) for parasympathetic nerve detection; substance P – SP (1:1000; mouse monoclonal antibody; ab14184, Abcam) and calcitonin gene-related peptide – CGRP (1:1000; rabbit monoclonal antibody; ab81887, Abcam) for sensory nerve detection. After incubation for 1 h at room temperature, the slides were incubated for 30 min with the secondary fluorescent antibodies, goat anti-rabbit Alexa Fluor 594 (1:200; Vector), and horse anti-mouse

Alexa Fluor 488 (1:200; Vector). Slides were then washed in the phosphate-buffered saline solution (PBS), mounted with Antifade Mounting Medium with 4,6-diamidino-2-phenylindole (DAPI) (Vector), and visualized using an Eclipse 80i microscope (Nikon).

Quantitative assessment of nerve proliferation. Selected representative specimens (n=5) from each group were stained with a combination of nerve protein S100 staining and proliferating cell nuclear antigen (PCNA) detection. Briefly, after antigen retrieval in citrate buffer, tissue sections were treated with 3% H₂O₂ for 5 min to quench endogenous peroxidases, then incubated with polyclonal rabbit anti-S100 antibody (1:800; Dako) for 1 h, washed in PBS, and incubated with alkaline phosphatase-conjugated goat anti-rabbit secondary antibody (Vector) for 30 min, the activity of which was developed with ImmPACT Vector Red (Vector). Slides were then coated with mouse anti-PCNA monoclonal antibody (1:200, Dako), incubated for 1 h at room temperature, and developed with peroxidase EnVision FLEX kit with diaminobenzidine (Agilent). Slides were counterstained with hematoxylin (BD Bamed, Czech Republic), mounted with Fluorescence Mounting medium (Agilent), and examined with an Eclipse 80i microscope (Nikon).

Statistical analysis. All statistical analyses were performed using GraphPad Prism Version 8 for Windows (GraphPad Software Inc.). The Shapiro-Wilk test was used to test the normality of the data. One-way ANOVA followed by Tukey's multiple comparison test was used to calculate statistical significance between groups. The relationship between innervation density and Gleason score was evaluated using linear regression and Pearson's correlation. Changes were considered statistically significant when p-values were <0.05. Data in graphs are expressed as mean ± SEM.

Results

Density of innervation in the healthy prostate, benign prostatic hyperplasia, and prostate cancer. The histomorphological evaluation of S100-positive nerve fibers revealed significantly lower nerve density in prostate cancer (PCa) specimens compared to the healthy prostate gland (CON) and benign prostatic hyperplasia (BH) (CON vs. PCa, p<0.05; BH vs. PCa, p<0.001). In addition, there was a higher density of nerves in BH compared to the healthy prostate, but the difference was not significant (CON vs. BH, p=0.27) (Figure 1A). We further divided the prostate cancer specimens into low-grade (LG PCa) and high-grade (HG PCa) based on the Gleason grading system. Similarly, the amount of S100-positive nerve fibers was significantly lower in LG PCa and HG PCa compared to CON and BH (CON vs. LG PCa, p<0.01; BH vs. LG PCa, p≤0.001; CON vs. HG PCa, p<0.05; BH vs. HG PCa, p<0.001) (Figure 1B). There was no statistically significant difference in the number of S100-positive nerve fibers between LG PCa and HG PCa (LG PCa vs. HG PCa, p=0.99).

Types of innervations in the healthy prostate, benign prostatic hyperplasia, and prostate cancer. Immunofluorescence performed on selected representative specimens revealed a high number of nerve fibers of various sizes in normal prostate (CON), and the number of nerves increased from the center to the periphery. The largest number of nerve fibers was recorded in the prostatic capsule, while only scattered nerve fibers were recorded between the glands and in the central periurethral region, and thicker nerve fibers were recorded toward the edge. Most of these small and large nerve fibers in CON were positive for the marker of sympathetic innervation, TH (Figure 2A). The majority of nerves in CON were not positive for VAcHT parasympathetic innervation, with only a small number of nerves localized between the glands and at peripheral parts of the prostate gland (Figure 2B). Virtually all CON specimens were negative for

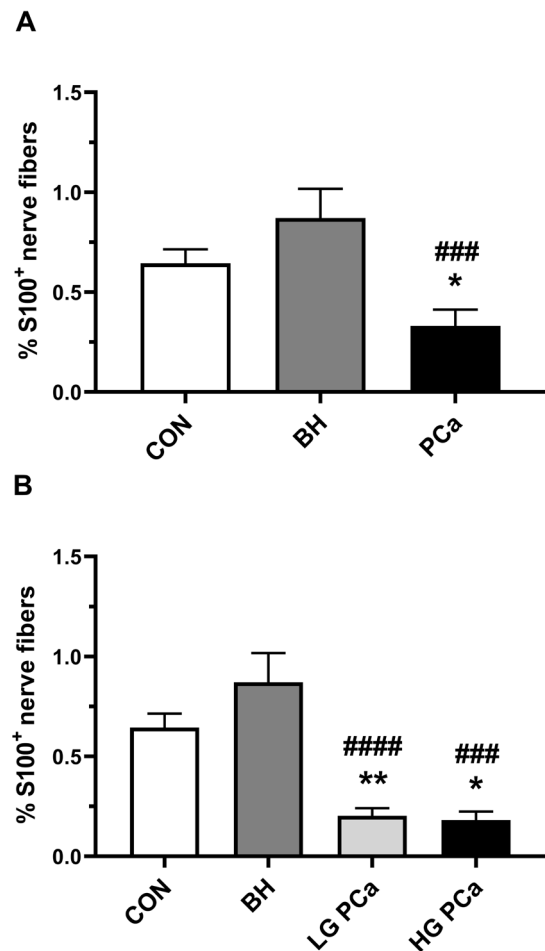


Figure 1. Density of innervation in different pathologies of the human prostate. Abbreviations: CON – healthy prostate gland; BH – benign prostatic hyperplasia; PCa – prostate cancer; LG PCa – low-grade prostate cancer; HG PCa – high-grade prostate cancer. The density of innervation represents the percentage of S100 positivity of the section surface. Values are expressed as mean ± SEM. Statistical significance between CON and PCa, CON and LG PCa, CON and HG PCa specimens: *p<0.05, **p<0.01. Statistical significance between BH and PCa, BH and LG PCa, BH and HG PCa: ###p<0.001, ####p<0.0001

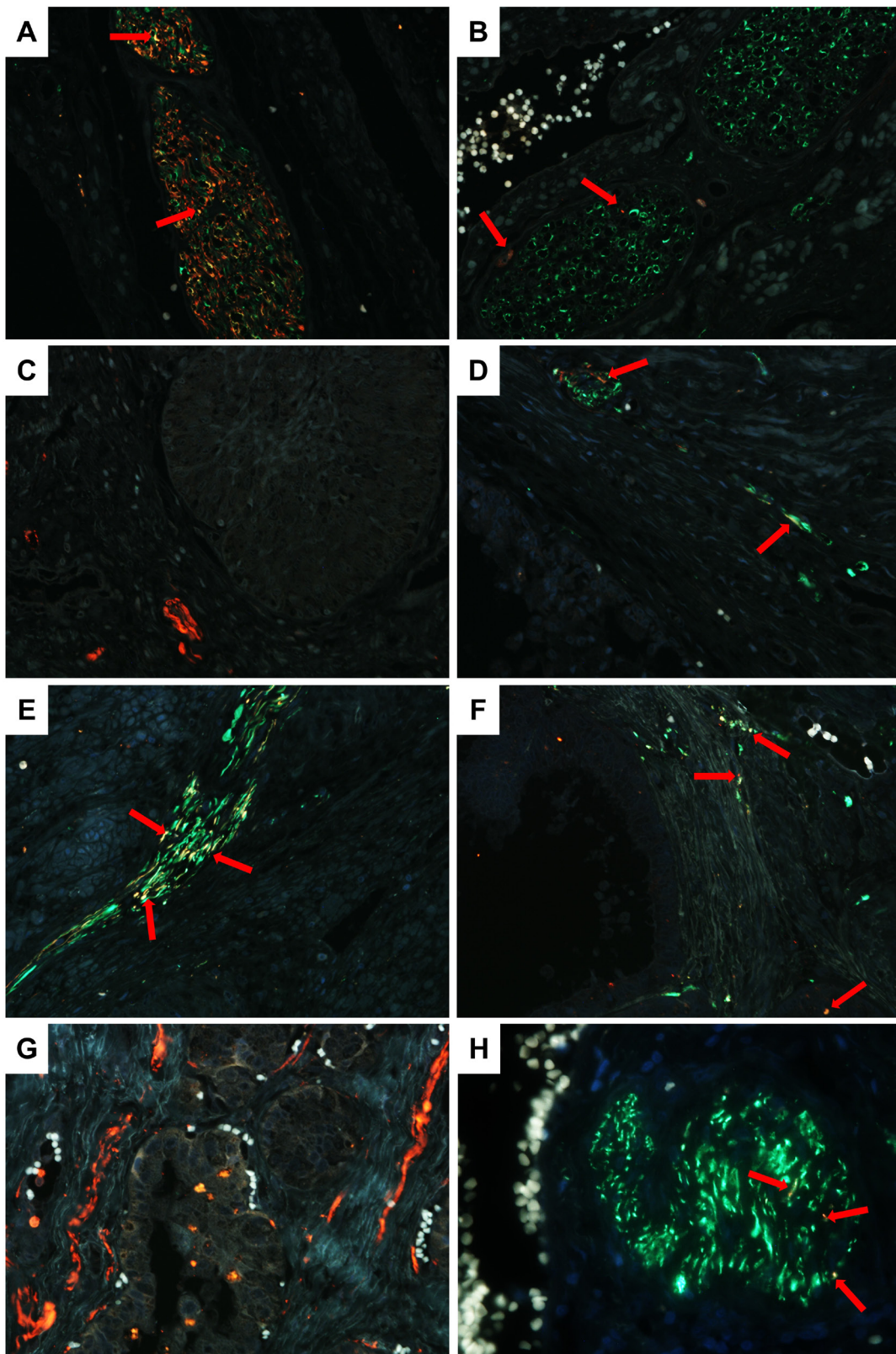


Figure 2. Determination of innervation types in healthy human prostate (A–D) and benign prostatic hyperplasia (E–H). A, E: sympathetic nerves (PGP9.5, green+TH, red); B, F: parasympathetic nerves (PGP9.5, green+VAcT, red); C, G: sensory nerves (S100, red+SP, green); D, H: sensory nerves (PGP9.5, green+CGRP, red). The presence of a specific type of innervation = areas of overlap = yellow-brown color (red arrows); 400×

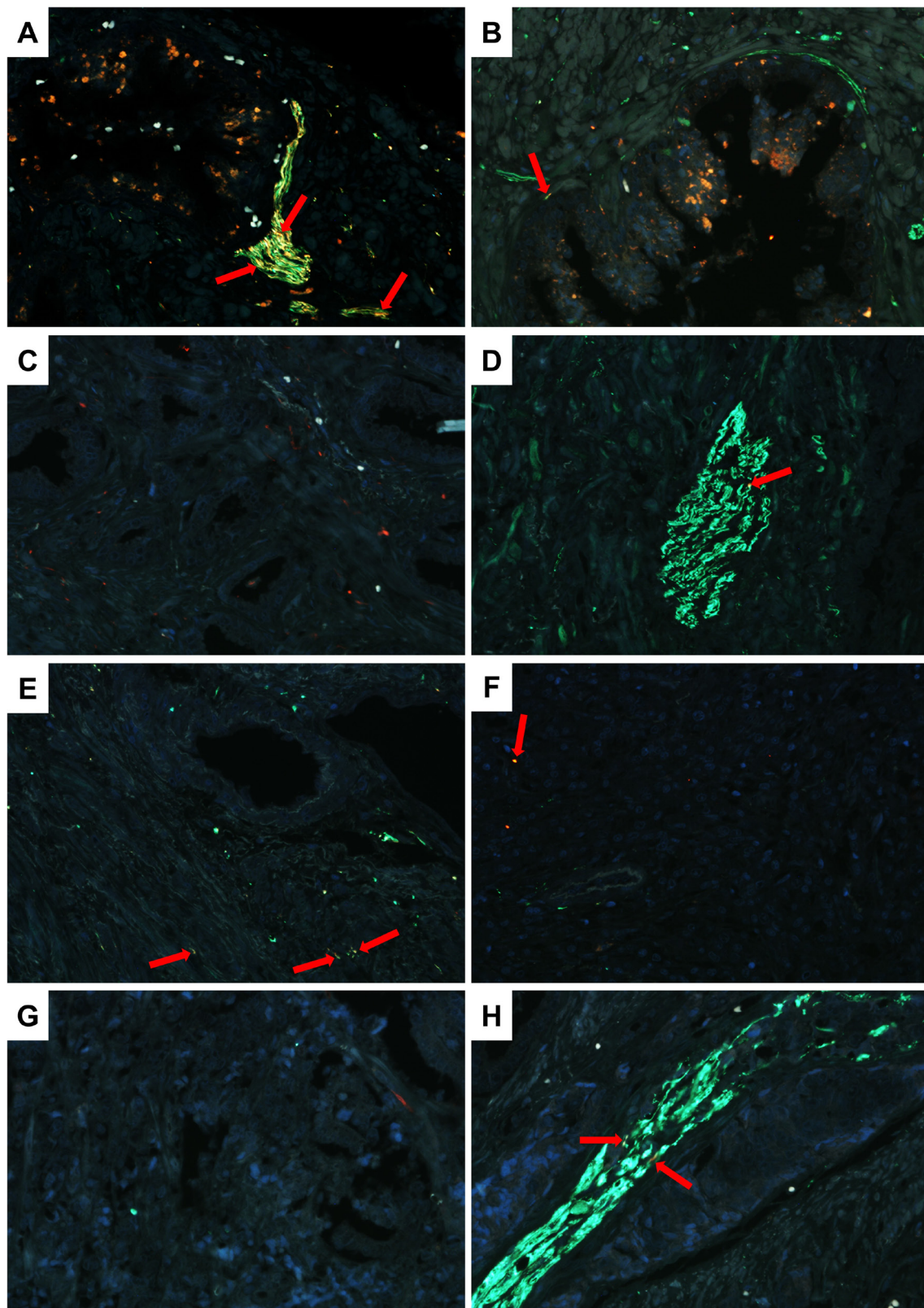


Figure 3. Determination of innervation types in human prostate carcinoma, low-grade (A–D), and high-grade (E–H). A, E: sympathetic nerves (PGP9.5, green+TH, red); B, F: parasympathetic nerves (PGP9.5, green+VAcHT, red); C, G: sensory nerves (S100, red+SP, green); D, H: sensory nerves (PGP9.5, green+CGRP, red). The presence of a specific type of innervation = areas of overlap = yellow-brown color (red arrows); 400×

the SP marker of sensory innervation (Figure 2C). CGRP-positive sensory innervation was found in several small nerve fibers and occasionally in larger nerve fibers in the periurethral region and between the prostatic glands (Figure 2D). In BH, similarly to CON, immunofluorescence revealed a relatively large number of small and large nerve fibers, whereas TH-positive sympathetic nerves were more prominent in the peripheral parts of hyperplastic nodules within larger nerve fibers (Figure 2E). Most of the BH specimens showed no parasympathetic marker positivity with only a few isolated fine nerve fibers (Figure 2F). Sensory innervation was not detected with SP in all BH specimens (Figure 2G), although, sporadic isolated CGRP-positive nerve fibers were found in 1/10 of particularly large nerves (Figure 2H). The pattern of innervation in prostate cancer was similar to that in healthy prostate and benign prostatic hyperplasia. However, the number of all nerve types was considerably lower in LG PCa, and even lower in HG PCa. The majority of the nerves were located at the edge of the tumors. Sympathetic nerve fibers were only sporadically present in the peripheral parts of the tumors (Figure 3A). Only a minimal number of nerve fibers (in about 1/10 nerves) showed positivity for the parasympathetic marker VAcHT (Figure 3B). There was almost no positivity for sensory innervation detected by SP (Figure 3C), except for occasional CGRP-positive fine fibers within larger nerves (Figure D). HG PCa showed only minimal amounts of nerve fibers compared to CON, BH, and LG PCa. At the periphery of the tumor infiltrate the amount of nerve fibers increased, although minimally. Several thin TH-positive sympathetic fibers were found at the periphery of the tumor, especially in the areas with perineural spread of the carcinoma (Figure 3E). Parasympathetic innervation was rarely detected only at the tumor periphery (Figure 3F). Almost all HG PCa specimens were negative for sensory innervation with SP, except for only two cases showing isolated fibers with CGRP positivity at the periphery of the tumors (Figure 3H).

The relationship between the density of innervation and Gleason score. Next, we evaluated the density of innervation,

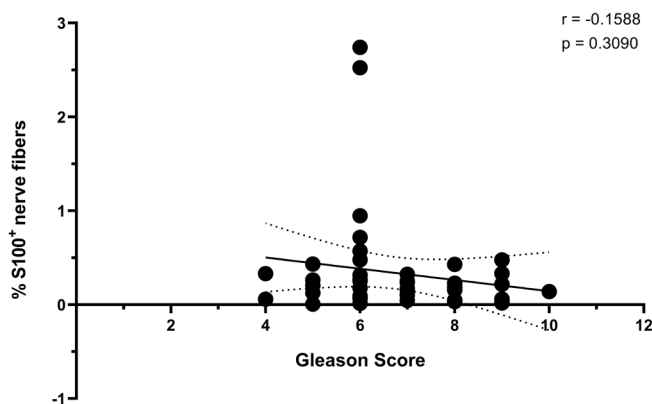


Figure 4. Association between the density of innervation and prostate cancer prognostic Gleason score.

represented by the area percentage of protein S100 positive nerve fibers in relation to the Gleason score using simple linear regression and Pearson's correlation. This evaluation has not shown any significant relationship between innervation density and Gleason score. However, the low innervation density in high-grade prostate cancer specimens found in our study indicates and supports the existence of this relationship ($r=-0.1588$, $p=0.3090$, Figure 4).

Quantitative analysis of nerve proliferation. Dual staining was used to identify nerve structures in red and nuclei with proliferative activity in brown color. For the quantitative analysis of nerve proliferation, we counted the number of PCNA-positive nuclei in S100-labeled nerve fibers on an area of 1 cm². This semiquantitative evaluation showed the highest average number (3.0/cm²) in CON and BH (1.4/cm²), less in LG PCa (1.1/cm²) and HG PCa (0.4/cm²).

Discussion

Cancer innervation by autonomic and sensory nerve fibers is now a widely accepted phenomenon that may be associated with enhanced cancer growth and metastasis in many types of tumors such as pancreatic [15, 16], gastric [17, 18], breast [19], colorectal [20], hepatocellular [9], lung cancer [21], and malignant melanoma [22, 23], including prostate cancer [7, 9, 17]. Cancer innervation is not limited to the process of perineural invasion but there is accumulating evidence of neural ingrowth into cancerous tissue induced by the synthesis and secretion of neurotrophic factors, axon guidance molecules, and exosomes in/from cancer cells, a process called neurogenesis [24, 25].

Available data suggests that prostate cancer innervation is necessary, especially in the early stages of tumor progression [7, 26]. Several experimental works have shown that the initiation and progression of prostate carcinoma are associated with functional adrenergic nerve signaling, which may be closely related to the induction of angiogenesis in the tumor [7, 26]. These assumptions are indirectly supported by other studies showing a decreased incidence of prostate cancer in humans with paraplegic denervation or pharmacologic β_2 -adrenergic inhibition [27, 28]. Experimental prostate denervation by local administration of botulotoxin resulted in reduced size of implanted prostate cancer. A human neoadjuvant clinical trial using local denervation of prostate cancer with botulotoxin before prostatectomy resulted in increased apoptosis of cancer cells [29].

In contrast to the above-cited works, our analysis showed that prostate cancer specimens had a significantly lower density of innervation compared to the healthy prostate gland and benign prostatic hyperplasia. Obviously, the result of innervation assessment in experimental prostate cancer models cannot be directly extrapolated to clinical situations in human patients. Interestingly, Magnon et al. [7] also reported a direct correlation between prostate cancer progression and density of innervation in their experimental

part of the study, however, their analysis of innervation in human prostate cancer showed a lower density in the tumor tissue, analogous to our results. Most of the nerves were localized at the edge or around the tumor.

Sympathetic nerves identified by their TH positivity were the most common nerve type observed in prostate cancer, and even more so in normal prostate and benign prostatic hyperplasia. These findings were consistent with the results of other studies [4, 26, 30], and support the notion of a tumor-promoting activity of adrenergic signaling in the prostate. Parasympathetic nerve fibers with VACHT positivity were less frequent in both neoplastic and nonneoplastic prostate tissue compared to the representation of the sympathetic nerve type. The results of the experimental studies indicated their role especially in the process of tumor propagation [7, 13], while the sympathetic type of nerves is predominantly involved in cancer initiation. The presence of innumerable sensory nerve fibers, mostly CGRP-positive, confirmed the involvement of these nerve types in the formation of the tumor microenvironment. Their role has been considered in the process of metastatic spread, especially in the development of bone marrow metastases [7, 31].

Zahalka et al. [26] demonstrated the role of adrenergic innervation in the progression of low-grade PIN to high-grade PIN and carcinoma in their experimental prostate cancer model. In the present study, we correlated the innervation density of prostate carcinoma with the prognostic value of the Gleason score. Although not significant, there was a negative correlation between innervation density and the value of the Gleason score. Other authors analyzed the expression of pro-nerve growth factor expression (proNGF) by prostate cancer cells and found a positive correlation between the proNGF expression and the Gleason score of the tumors. This study demonstrated the potential of the prostate cancer cells to stimulate nerve outgrowth in the tumor microenvironment but was not complemented by documentation of nerve density changes in the tumors [32].

To shed more light on the question of the possible proliferation of nerve structures in the prostate carcinoma microenvironment, we attempted to detect proliferative activity in the tumor nerve fibers. Since the half-life of the Ki-67 protein is only 90 min short [33], we decided to use the detection of proliferating cell nuclear antigen (PCNA) protein, which has a longer survival time in the cells [34]. The low number of PCNA-positive nuclei in the nerves within the prostate cancer tissue was not surprising, as this correlated with the low density of the nerves in the tumor. Based on our findings, we suggested that the lower density of all nerve types in the tumor specimens may be a consequence of the expansive tumor growth and the hypoxic tumor microenvironment, which cannot be excluded [35, 36]. Similar results were confirmed by Sigorski et al. [14], who showed significantly lower PGP9.5 and TH nerve density in the human prostate cancer compared to the benign prostatic hyperplasia specimens, and conversely, higher nerve density in the tumor

surrounding areas and at the tumor invasive front. Similar negative correlations between low tumor nerve density and poor prognosis have also been reported in pancreatic and gastric cancers [37, 38].

Several prostate cancer studies have reported that higher nerve density is associated with a worse prognosis. Brundl et al. [39] showed that prostate cancer resulted in a significantly higher number of capsular nerves. Furthermore, increased nerve density in the prostate correlated with increased tumor spread to regional lymph nodes [12]. A high density of sympathetic innervation was also associated with the development of metastases and castration-resistant prostate cancer [3]. The low density of innervation in prostate cancer specimens demonstrated in our study and the differences from the results of other authors point to the complexity of the processes associated with tumor progression and highlight the need for further research that should clarify the distribution of nerve fibers in prostate cancer.

In conclusion, our results revealed a significantly lower density of nerves in the prostate cancer specimens, with the most represented sympathetic nerve fibers located predominantly in the peripheral parts of the tumor. Parasympathetic nerve fibers were identified in only about 10% of the nerves, while sensory nerves were virtually absent. These results are consistent with the findings of several other studies of human prostate cancer. Obviously, results from experimental prostate cancer models can be extrapolated only to a limited extent to human pathology. The relationship between the extent of innervation and the biology of prostate cancer is very complex and will require more detailed information to be applied to therapeutic solutions.

Acknowledgments: This work was supported by the Slovak Research and Development Agency (APVV-17-0090) and the Slovak Research Agency (VEGA 1/0684/21).

References

- [1] SUNG H, FERLAY J, SIEGEL RL, LAVERSANNE M, SOERJOMATARAM I et al. Global Cancer Statistics 2020: GLOBOCAN Estimates of Incidence and Mortality Worldwide for 36 Cancers in 185 Countries. *CA Cancer J Clin* 2021; 71: 209–249. <https://doi.org/10.3322/caac.21660>
- [2] SIEGEL RL, MILLER KD, FUCHS HE, JEMAL A. Cancer statistics, 2022. *CA Cancer J Clin* 2022; 72(1): 7–33. <https://doi.org/10.3322/caac.21708>
- [3] DWIVEDI S, BAUTISTA M, SHRESTHA S, ELHASASNA H, CHAPHEKAR T et al. Sympathetic signaling facilitates progression of neuroendocrine prostate cancer. *Cell Death Discov* 2021; 7: 364. <https://doi.org/10.1038/s41420-021-00752-1>
- [4] SIGORSKI D, WESOŁOWSKI W, GRUSZECKA A, GULCZYNSKI J, ZIELINSKI P et al. Neuropeptide Y and its receptors in prostate cancer: associations with cancer invasiveness and perineural spread. *J Cancer Res Clin Oncol* 2023; 149: 5803–5822. <https://doi.org/10.1007/s00432-022-04540-x>

- [5] WHITE CW, XIE JH, VENTURA S. Age-related changes in the innervation of the prostate gland: implications for prostate cancer initiation and progression. *Organogenesis* 2013; 9: 206–215. <https://doi.org/10.4161/org.24843>
- [6] AYALA GE, WHEELER TM, SHINE HD, SCHMELZ M, FROLOV A et al. In vitro dorsal root ganglia and human prostate cell line interaction: redefining perineural invasion in prostate cancer. *Prostate* 2001; 49: 213–223. <https://doi.org/10.1002/pros.1137>
- [7] MAGNON C, HALL SJ, LIN J, XUE X, GERBER L et al. Autonomic nerve development contributes to prostate cancer progression. *Science* 2013; 341: 1236361. <https://doi.org/10.1126/science.1236361>
- [8] YE Y, XIE T, AMIT M. Targeting the Nerve-Cancer Circuit. *Cancer Res* 2023; 83: 2445–2447. <https://doi.org/10.1158/0008-5472.CAN-23-1754>
- [9] ZHANG L, WU LL, HUAN HB, CHEN XJ, WEN XD et al. Sympathetic and parasympathetic innervation in hepatocellular carcinoma. *Neoplasma* 2017; 64: 840–846. https://doi.org/10.4149/neo_2017_605
- [10] MRAVEC B. Neurobiology of cancer: Definition, historical overview, and clinical implications. *Cancer Med* 2022; 11: 903–921. <https://doi.org/10.1002/cam4.4488>
- [11] ALI SR, JORDAN M, NAGARAJAN P, AMIT M. Nerve Density and Neuronal Biomarkers in Cancer. *Cancers (Basel)* 2022; 14: 4817. <https://doi.org/10.3390/cancers14194817>
- [12] OLAR A, HE D, FLORENTIN D, DING Y, AYALA G. Biologic correlates and significance of axonogenesis in prostate cancer. *Hum Pathol* 2014; 45: 1358–1364. <https://doi.org/10.1016/j.humpath.2014.02.009>
- [13] REEVES FA, BATTYE S, ROTH H, PETERS JS, HOVENS C et al. Prostatic nerve subtypes independently predict biochemical recurrence in prostate cancer. *J Clin Neurosci* 2019; 63: 213–219. <https://doi.org/10.1016/j.jocn.2019.01.052>
- [14] SIGORSKI D, GULCZYNSKI J, SEJDA A, ROGOWSKI W, IZYCKA-SWIESZEWSKA E. Investigation of Neural Microenvironment in Prostate Cancer in Context of Neural Density, Perineural Invasion, and Neuroendocrine Profile of Tumors. *Front Oncol* 2021; 11: 710899. <https://doi.org/10.3389/fonc.2021.710899>
- [15] BRESSY C, LAC S, NIGRI J, LECA J, ROQUES J et al. LIF Drives Neural Remodeling in Pancreatic Cancer and Offers a New Candidate Biomarker. *Cancer Res* 2018; 78: 909–921. <https://doi.org/10.1158/0008-5472.CAN-15-2790>
- [16] RENZ BW, TAKAHASHI R, TANAKA T, MACCHINI M, HAYAKAWA Y et al. beta2 Adrenergic-Neurotrophin Feed-forward Loop Promotes Pancreatic Cancer. *Cancer Cell* 2018; 33: 75–90 e7. <https://doi.org/10.1016/j.ccell.2017.11.007>
- [17] ZHAO CM, HAYAKAWA Y, KODAMA Y, MUTHUPALANI S, WESTPHALEN CB et al. Denervation suppresses gastric tumorigenesis. *Sci Transl Med* 2014; 6: 250ra115. <https://doi.org/10.1126/scitranslmed.3009569>
- [18] HAYAKAWA Y, SAKITANI K, KONISHI M, ASFAHA S, NIIKURA R et al. Nerve Growth Factor Promotes Gastric Tumorigenesis through Aberrant Cholinergic Signaling. *Cancer Cell* 2017; 31: 21–34. <https://doi.org/10.1016/j.ccell.2016.11.005>
- [19] ZHAO Q, YANG Y, LIANG X, DU G, LIU L et al. The clinicopathological significance of neurogenesis in breast cancer. *BMC Cancer* 2014; 14: 484. <https://doi.org/10.1186/1471-2407-14-484>
- [20] KUOL N, DAVIDSON M, KARAKKAT J, FILIPPONE RT, VEALE M et al. Blocking Muscarinic Receptor 3 Attenuates Tumor Growth and Decreases Immunosuppressive and Cholinergic Markers in an Orthotopic Mouse Model of Colorectal Cancer. *Int J Mol Sci* 2022; 24: 596. <https://doi.org/10.3390/ijms24010596>
- [21] SHAO JX, WANG B, YAO YN, PAN ZJ, SHEN Q et al. Autonomic nervous infiltration positively correlates with pathological risk grading and poor prognosis in patients with lung adenocarcinoma. *Thorac Cancer* 2016; 7: 588–598. <https://doi.org/10.1111/1759-7714.12374>
- [22] KESKINOV AA, TAPIAS V, WATKINS SC, MA Y, SHURIN MR et al. Impact of the Sensory Neurons on Melanoma Growth In Vivo. *PLoS One* 2016; 11: e0156095. <https://doi.org/10.1371/journal.pone.0156095>
- [23] PRAZERES P, LEONEL C, SILVA WN, ROCHA BGS, SANTOS GSP et al. Ablation of sensory nerves favours melanoma progression. *J Cell Mol Med* 2020; 24: 9574–9589. <https://doi.org/10.1111/jcmm.15381>
- [24] ENTSCHLADEN F, PALM D, LANG K, DRELL TLT, ZAENKER KS. Neoneurogenesis: tumors may initiate their own innervation by the release of neurotrophic factors in analogy to lymphangiogenesis and neoangiogenesis. *Med Hypotheses* 2006; 67: 33–35. <https://doi.org/10.1016/j.mehy.2006.01.015>
- [25] MARCH B, FAULKNER S, JOBLING P, STEIGLER A, BLATT A et al. Tumour innervation and neurosignalling in prostate cancer. *Nat Rev Urol* 2020; 17: 119–130. <https://doi.org/10.1038/s41585-019-0274-3>
- [26] ZAHALKA AH, ARNAL-ESTAPE A, MARYANOVICH M, NAKAHARA F, CRUZ CD et al. Adrenergic nerves activate an angio-metabolic switch in prostate cancer. *Science* 2017; 358: 321–326. <https://doi.org/10.1126/science.aah5072>
- [27] FRISBIE JH, BINARD J. Low prevalence of prostatic cancer among myelopathy patients. *J Am Paraplegia Soc* 1994; 17: 148–149. <https://doi.org/10.1080/01952307.1994.11735926>
- [28] OZLER S, PAZARCI P. Anti-tumoral effect of beta-blockers on prostate and bladder cancer cells via mitogen-activated protein kinase pathways. *Anticancer Drugs* 2022; 33: 384–388. <https://doi.org/10.1097/CAD.0000000000001271>
- [29] COARFA C, FLORENTIN D, PUTLURI N, DING Y, AU J et al. Influence of the neural microenvironment on prostate cancer. *Prostate* 2018; 78: 128–139. <https://doi.org/10.1002/pros.23454>
- [30] ZHOU M, PATEL A, RUBIN MA. Prevalence and location of peripheral nerve found on prostate needle biopsy. *Am J Clin Pathol* 2001; 115: 39–43. <https://doi.org/10.1309/2APJ-YKBD-97EH-67GW>
- [31] JIMENEZ-ANDRADE JM, BLOOM AP, STAKE JI, MANTYH WG, TAYLOR RN et al. Pathological sprouting of adult nociceptors in chronic prostate cancer-induced bone pain. *J Neurosci* 2010; 30: 14649–14656. <https://doi.org/10.1523/JNEUROSCI.3300-10.2010>

- [32] PUNDAVELA J, DEMONT Y, JOBLING P, LINCZ LE, ROSELLI S et al. ProNGF correlates with Gleason score and is a potential driver of nerve infiltration in prostate cancer. *Am J Pathol* 2014; 184: 3156–3162. <https://doi.org/10.1016/j.ajpath.2014.08.009>
- [33] HEIDEBRECHT HJ, BUCK F, HAAS K, WACKER HH, PARWARESCH R. Monoclonal antibodies Ki-S3 and Ki-S5 yield new data on the 'Ki-67' proteins. *Cell Prolif* 1996; 29: 413–425. <https://doi.org/10.1111/j.1365-2184.1996.tb00984.x>
- [34] BRAVO R, MACDONALD-BRAVO H. Existence of two populations of cyclin/proliferating cell nuclear antigen during the cell cycle: association with DNA replication sites. *J Cell Biol* 1987; 105: 1549–1554. <https://doi.org/10.1083/jcb.105.4.1549>
- [35] MAUFFREY P, TCHITCHEK N, BARROCA V, BEMELMANS AP, FIRLEJ V et al. Progenitors from the central nervous system drive neurogenesis in cancer. *Nature* 2019; 569: 672–678. <https://doi.org/10.1038/s41586-019-1219-y>
- [36] JUNG E, ALFONSO J, MONYER H, WICK W, WINKLER F. Neuronal signatures in cancer. *Int J Cancer* 2020; 147: 3281–3291. <https://doi.org/10.1002/ijc.33138>
- [37] IWASAKI T, HIRAOKA N, INO Y, NAKAJIMA K, KISHI Y et al. Reduction of intrapancreatic neural density in cancer tissue predicts poorer outcome in pancreatic ductal carcinoma. *Cancer Sci* 2019; 110: 1491–1502. <https://doi.org/10.1111/cas.13975>
- [38] BAE GE, KIM HS, WON KY, KIM GY, SUNG JY et al. Lower Sympathetic Nervous System Density and beta-adrenoreceptor Expression Are Involved in Gastric Cancer Progression. *Anticancer Res* 2019; 39: 231–236. <https://doi.org/10.21873/anticancerres.13102>
- [39] BRUNDL J, SCHNEIDER S, WEBER F, ZEMAN F, WIELAND WF et al. Computerized quantification and planimetry of prostatic capsular nerves in relation to adjacent prostate cancer foci. *Eur Urol* 2014; 65: 802–808. <https://doi.org/10.1016/j.eururo.2013.04.043>